PROCEEDINGS, 48th Workshop on Geothermal Reservoir Engineering
Stanford University, Stanford, California, February 6-8, 2023
SGP-TR-224

Permeability enhancement process by shear slip on existing fractures from the microseismic perspective

Yusuke Mukuhira, Takuya Ishibashi, Takatoshi Ito, Hiroshi Asanuma

Institute of Fluid Science, Tohoku University, 2-1-1 Katahira, Aoba-ku, Sendai, 980-8577

mukuhira@tohoku.ac.jp

Keywords: Microseismicity, permeability, shear slip, fracture

ABSTRACT

As a key physical phenomenon of Enhanced Geothermal System (EGS) development, shear slip on existing fracture enhances its permeability. Previous laboratory and numerical works presented that permeability enhancement occurs in a direction perpendicular to the shear slip direction by dilation on the fracture surface (e.g., Yeo et al., 1998). This is attributed to the accumulation of distributed contact areas, which results in the development of channeling flow on fracture (e.g., Watanabe et al., 2008). We relied on these phenomena in the interpretation of microseismic observations, such as hypocenter migration in EGS fields (Evans et al., 2005; Mukuhira et al., 2016). However, a recent laboratory study suggests permeability enhancement by shear slip is not significantly visible (Ishibashi. et al., 2021). Therefore, this study analyzed the permeability enhancement on a field scale using the microseismicity information at hydraulic stimulation. In this study, we picked up the microseismic data of EGS development in Basel, Switzerland, and analyzed the direction of shear slip from the orientation of fault and in-situ stress information. We chose the group of events that occurred from one macroscopic fracture. We evaluate the shear slip direction from the geomechanical analysis and compare it with the overall microseismic evolution direction to investigate the directional effect of shear slip on permeability enhancement. Then, we analyze inter-event time and inter-event distance as a proxy of pore pressure migration velocity. Based on the observations from these analyses, we discuss the effect of permeability enhancement by shear slip and its orientation in comparison with the shear slip direction.

1. INTRODUCTION

Shear failure on existing fractures or faults enhances the permeability of fractures or faults. This is a well-known permeability enhancement process where fracture apertures increase with shear displacement. This is the basis of various geomechanical problems, including Enhanced Geothermal System (EGS) development. Therefore, hydraulic stimulation to cause shear slip is often used in EGS, aiming for the enhancement of permeability in the reservoir. The permeability enhancement along with shear slip occurs heterogeneously on the fracture due to the distribution of contact points and redistribution associated with shear displacement. Shear slip made fracture more permeable in the direction perpendicular to the displacement (e.g., Yeo et al., 1998), which results in the accumulation of channeling flow (e.g., Watanabe et al., 2008). A similar concept has been proposed to describe the growth of seismic swarm behavior (e.g., Sibson, 1996). Some field studies (Evans et al., 2005; Mukuhira et al., 2016) used this phenomenon to interpret the observations related to permeability enhancement through microseismicity. However, a recent laboratory study reported the new observations that permeability enhancement by shear slip is not evident from permeability measurement in shear displacement under confining pressure conditions (Ishibashi. et al., 2021). In addition, some numerical work also suggested that the injectivity increase cannot be explained only with permeability enhancement by shear slip and that some mix-mode (shear and opening) or opening fracture should have contributed permeability enhancement process (McClure and Horne, 2014; Norbeck et al., 2018). Therefore, permeability enhancement by shear slip in field scale is still open question. We study the permeability enhancement process by the shear slip on a larger scale, using microseismic information. This study used the microseismicity and in-situ stress information from the Basel EGS project in Switzerland and explored the evidence of 1) perpendicular relation between shear slip and permeability enhancement and 2) permeability enhancement throughout the microseismic analysis. First, we estimate the macroscopic structure from microseismic clustering analysis and estimate the direction of shear slip on that structure with in-situ stress information. We investigate the directional relationship between shear slip and microseismicity migration as a proxy of pore pressure. Subsequently, we also investigated the microseismic evidence of permeability enhancement by shear failure.

2. DATA AND METHODOLOGY

2.1 Microseismic data

We use the well-recorded microseismicity at the hydraulic stimulation of Basel EGS development in 2006 (Häring et al., 2008). Geothermal Explorers Ltd., the operator of the Basel EGS project (GEL), deployed six borehole station depths ranging from 2265m to near the surface. Our previous works determined the absolute locations of hypocenters for around 3000 microseismic events with manual pick and a 1D velocity model (Asanuma et al., 2007). Then, Asanuma et al. (2008) relocated hypocenters with refined pick by waveform similarity evaluation. A series of relocation processes included microseismic clustering, where similar and closer microseismic events are grouped and identified clusters. A microseismic cluster often delineates macro or microscopic structure in the reservoir according to the method of clustering. Our refined seismic catalog has two versions. The catalog of the first version consists of the clustering result where waveform similarity is evaluated in 1~60 Hz. These clusters correspond to the macroscopic fractures as the cluster tends to be bigger scale (100~ m) compared to another version of the catalog that is microscopic structures are identified by a higher frequency band (40-97 Hz)

(Mukuhira et al., 2021). We utilized this macroscopic fracture information (Figure 1) for this research and chose several clusters showing clear fracture planes and clear microseismic evolution in time and space. The dimension of this fracture was extracted by principal component analysis.

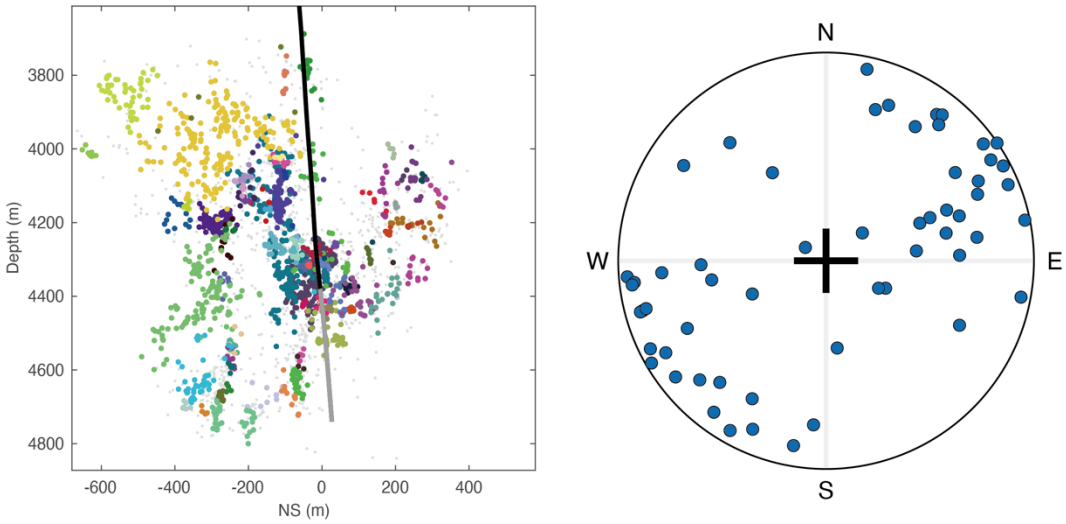

Figure 1: Clustered microseismic distribution in the lower frequency band (1-60 Hz) along the NS cross-section. The colored groups correspond to the microseismic clusters. The black line is the injection well trajectory, and the gray line is the open-hole section. Lower hemisphere plot of cluster poles.

2.2 In-situ stress data

To evaluate the orientation of the slip vector, we use the in-situ stress information from borehole logging data analysis and well-test results (Valley and Evans, 2019). The in-situ stress model consists as follows,

$$S_{\mathrm{Hmax}} = 5z + 90 \tag{1}$$

$$S_V = 24.9z \tag{2}$$

$$S_{\mathrm{hmin}} = 7z + 42 \tag{3}$$

where S_{Hmax} is the maximum horizontal stress (MPa), S_v is the vertical stress (MPa), S_{hmin} is the minimum horizontal stress (MPa), and z is the depth in km. We assumed hydrostatic conditions and resolved the orientation of the slip vector. The slip vector is defined as the orientation of maximum shear stress on the plane based on the assumption of the Wallace-Bott criterion (Wallace, 1951; Bott, 1959). Slip vectors were computed from the normal vector (pole vector) of faults and in-situ stress (Zoback, 2007).

2.3 Source radius

We also estimated the source radius for each event in clusters assuming the circler crack model (Eshelby, 1957) to check the overlap of the rapture area, which is also regarded as a permeability enhancement area. The source radius can be computed with equation (4) for each event using observed seismic moment M_o,

$$r = \left(\frac{7}{16}\frac{M_o}{\Delta\tau}\right)^{\frac{1}{3}} \tag{4}$$

where r is the source radius, and $\Delta\tau$ is the stress drop, for which we use the constant and representative value as 3 MPa.

3. RESULTS

3.1 Shear slip direction and microseismic cluster nucleation direction

First, we compare the shear slip direction and microseismic cluster nucleation direction. In Figure 2, we selected the cases of three macroscopic clusters (Cluster ID:1, 2, 26), where the number of events for the three clusters are 200, 245, and 118, respectively. Clusters 1 and 2 are the largest population clusters, and they delineate macroscopic vertical structures. Resolved slip vector is more or less a vertical trend, including a bit up dip component. The microseismic activity of cluster 1 generally starts from the shallower part, and it migrated to the deeper part, and we can see a clear migration trend from shallow to deep. There is clear perpendicular relationship between slip vectors and direction of event migration. Meanwhile, the migration trend of cluster 2 is more random, but there might be a weak trend of upward migration. At least, the longer direction of cluster 2 and the slip vector are perpendicular to each other. Cluster 26 also shows a clear

bilateral migration trend to a shallower and deeper direction and overall perpendicular relation to the slip vector orientations. Thus, we found the cases that exhibited the perpendicular trend between the shear slip direction and microseismic migration, i.e., pore pressure migration.

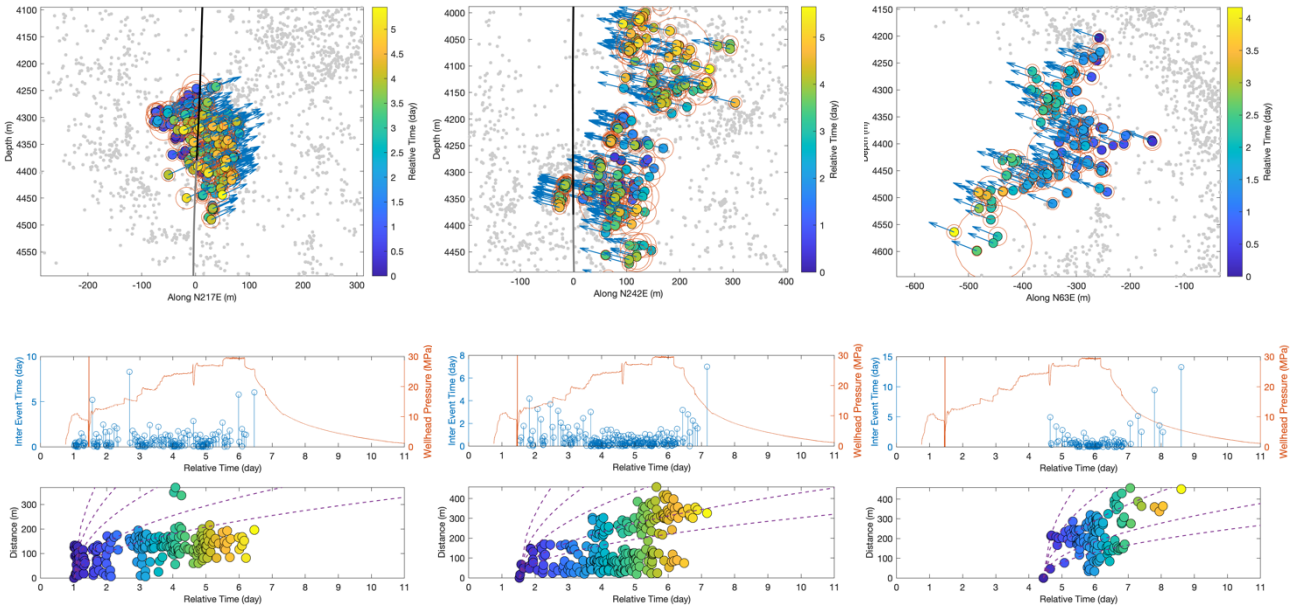

Figure 2: Relationship between slip vectors and microseismic cluster nucleation. The top row corresponds to three (1, 2, and 26) specific cluster cases of cross sections along their strikes. The color of the dots corresponds to the relative occurrence time within each cluster. Each blue arrows indicate the slip vectors of each event estimated from in-situ stress and structure dimension. The middle row shows inter-event time to the nearest preceding event within each cluster, compared with wellhead pressure. The lower row shows the time-1D distance plot (r-t plot) for each cluster. Broken lines are diffusion pore pressure front corresponding to the reference diffusivity set (0.01, 0.02, 0.05, 0.1, and 0.2 m^2/s)

Cluster 13 shows the counter observations (Figure 3) against the aforementioned observations. Cluster 13 exhibits clear horizontal microseismic migration outward of the reservoir, and its direction is nearly consistent with the slip vector for the structure of cluster 13. Modeled diffusivity for the microseismic migration of cluster 13 is around 0.1 m^2/s, which is significantly smaller than those for clusters 1, 2, and 26.

We also investigated the relationship in other clusters; however, we were not able to find such clear observations, partly because the population of other clusters is not very large even though the lower frequency-based clustering cases (Figure 4). There are not so many clusters consisted by of 100 events, and thus, it is hard to find such significant observations. We calculated the differential angle between averaged slip vector and cluster longer direction estimated by principal component analysis on the microseismic distribution (Figure 4 top). The differential angle distribution did not show any clear trends, and again, many clusters do not have enough events to satisfy the robustness of these kinds of analysis.

3.2 Permeability enhancement by a shear slip from the microseismic perspective

We investigated the proxy of permeability enhancement by shear slip using microseismic information. We assume that if the permeability of the fracture is enhanced by shear slip, more fluid flow occurs in the fracture, and it should deliver the pore pressure further and more quickly. Thus, we can expect more intense microseismicity activity as shear slip on the fracture happens. First, we plot the source radius estimated from equation (4) in Figure 2. Source radius defines the rupture area by shear slip, so it can be the area of permeability enhancement. For all three cases, we can observe that the source radius is overlapped with the neighboring event's hypocenter. The hypocenters of the events are often included in the permeability enhanced area. Next, we evaluate the inter-event time (time lag since the nearest preceding event) in the time series (Figure 2 middle row). For clusters 2 and 26, we observed reductions in inter-event time according to the stimulation. In addition, we, interestingly, also observed that inter-event time increased after the stop of stimulation. Note that we don't consider the spatial relation in this analysis, although the inter-event time between neighboring events should be evaluated. This point will be considered in a future study with the introduction of the channeling distribution model. Subsequently, microseismic event migration as a proxy of pore pressure migration is modeled with a linear diffusion model (Shapiro, 1997). The diffusion model is often used to model entire microseismic activity associated with fluid injection, but we can still use it for diffusion-like pore pressure migration in one single fracture. We plot the 1D time evolution from the first event in the cluster (Figures 2 and 3 bottom row) and evaluate the fit with the pressure front of several diffusivities (0.01, 0.02, 0.05, 0.1, and 0.2). If the permeability enhancement is significant, the fit with those pressure fronts would be varied later in the stimulation process. For all cases, the 1D time evolution of microseismic evolution falls in one envelop line of pressure front, and no significant excess of the 1D time evolution was observed. Visual inspection of fits for

each cluster suggests the best diffusivity, which can be translated to permeability, can differ for each cluster and the best diffusivity for cluster 13, which the slip vector and direction of event migration are parallel, is lower than those of the others.

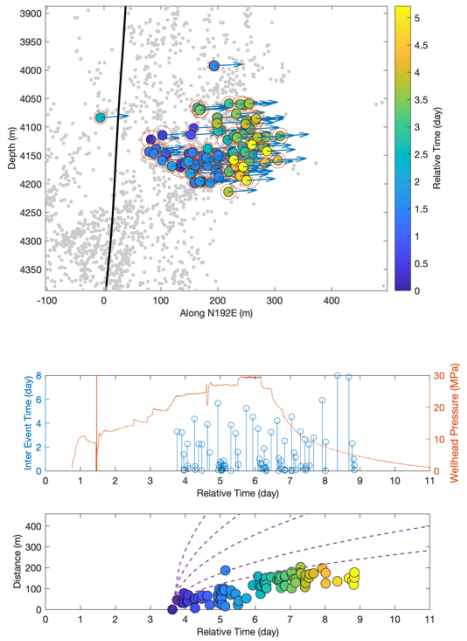

Figure 3: Counter observations from cluster 13 for the relationship between slip vectors and microseismic cluster nucleation. The figure is in the same format as Figure 2.

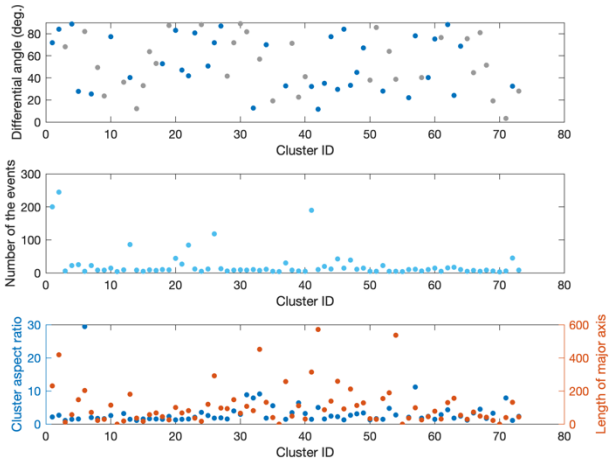

Figure 4: Summary of slip vector and microseismic migration trend. The top is the differential angle for all clusters. Grey dots correspond to the cluster that does not consist of 5 events. The middle is the number of events for each cluster. Low is the aspect ratio of the cluster shape (blue) and the maximum size of the cluster (red).

4. DISCUSSION

We observed that microseismic activity expanded to the direction perpendicular to the shear vector of preceding microseismicity. This observation suggests that permeability in that direction is preferentially enhanced as previous studies observed in laboratory scale or numerical simulation (Yeo et al., 2009; Watanabe et al., 2008). Therefore, permeability enhancement perpendicular to the shear slip direction is likely evident. At least the heterogeneity in permeability on the fracture exists. These observations also support the scale-up discussion of channeling flow in rough surface fracture (Ishibashi et al., 2016) and conceptual prediction (Sibson, 1996). However, we had counter observations of cluster 13, where the microseismic event expansion occurred along the shear vector. This observation seems

to contradict the previous observations, but the best-fitted diffusivity is lower than in other cases. This fact suggests that the fluid flow perpendicular to the shear vector was interrupted for some reason, and only fluid flow along the shear vector occurs. The shape of the microseismic cluster 13 is more circular than the elliptic shape of clusters 1,2, and 26.

We observed indirect evidence of permeability enhancement, which is the reduction of inter-event time along with the occurrence of microseismic events. But this analysis did not take care of the spatial relation between the preceding events, which requires the improvement of the analysis approach. The 1D microseismic distribution fit with one single diffusion pressure front and did not exceed the pressure front later, which permeability enhancement is expected. This observation suggests that there is no significant increase in permeability. Another possibility is that the permeability enhancement is so tiny that such macroscopic analysis of the diffusion model was not able to detect a permeability increase.

5. CONCLUSION

We tested two working hypotheses of permeability enhancement by shear slip on an existing fracture from a microseismic point of view. 1) perpendicular relation between shear slip direction and direction of permeability enhancement and 2) permeability enhancement. We studied the microseismic data set of the Basel EGS field. Microseismic cluster information is used to estimate the shear vector with the in-situ stress model and compared with the direction of cluster migration.

We observed that microseismicity migrated perpendicular to the shear vector for some clusters. Inter-event time in those clusters declined with the occurrence of microseismicity, and this is one of the indirect evidence of permeability enhancement. We conclude that the permeability enhancement is likely to occur in a perpendicular direction to the shear slip as we observed on a laboratory scale and permeability heterogeneity on the fault is also evident. We also observed that the other cluster showed the opposite behavior that microseismicity migrated along the shear vector, but the best fitted diffusivity for the event migration on that cluster was lower than others. There should be another factor to control the direction of permeability enhancement.

The permeability enhancement is not always obvious or less significant to be observed by microseismic behavior. We will introduce a fracture roughness model to fit observed microseismic distribution and channeling flow path distribution. Then, a more realistic inter-event time or fluid migration velocity will be estimated to discuss the permeability enhancement in more detail.

ACKNOWLEDGMENT

We thank Geo Explorers Ltd. and Geo-Energie Suisse AG for providing the microseismic wave data sets.

REFERENCES

Bott, M. H.: The mechanics of oblique slip faulting, Geological Magazine., 96, (1959), 109–117.

Evans, K. F.: Permeability creation and damage due to massive fluid injections into granite at 3.5 km at Soultz: 2. Critical stress and fracture strength, Journal of Geophysical Research B Solid Earth, 110, (2005), 1–14.

Häring, M. O., Schanz, U., Ladner, F., and Dyer, B. C.: Characterisation of the Basel 1 enhanced geothermal system, Geothermics 37, (2008), 469–495.

Ishibashi, T., Watanabe, N., Asanuma, H. and Tsuchiya, N.: Linking microearthquakes to fracture permeability change: The role of surface roughness, Geophysical Research Letters, 43, (2016), 7486–7493.

Ishibashi, T., Asanuma, H., and Watanabe, N.: Dynamics of Natural Rock Fractures in the EGS Revealed Via the Pressurized Water Injection Experiments in Laboratory, Proceedings World Geothermal Congress 2020+1, Reykjavik, Iceland, April - October 2021 (2021).

McClure, M. W. and Horne, R. N.: An investigation of stimulation mechanisms in Enhanced Geothermal Systems, International Journal Rock Mechanics and Mining Sciences. 72, (2014), 242–260.

Mukuhira, Y., Dinske, C., Asanuma, H., Ito, T., and Häring, M. O.: Pore pressure behavior at the shut-in phase and causality of large induced seismicity at Basel, Switzerland, Journal of Geophysical Research Solid Earth, 122, (2017), 411–435.

Mukuhira, Y., Fehler, M. C., Ito, T., Asanuma, H., and Häring, M. O. Injection-induced seismicity size distribution dependent on shear stress, Geophysical Research Letters, 48, (2021), e2020GL090934. https://doi. org/10.1029/2020GL090934.

Norbeck, J. H., McClure, M. W. and Horne, R. N.: Field observations at the Fenton Hill enhanced geothermal system test site support mixed-mechanism stimulation, Geothermics 74, (2018), 135–149.

Shapiro, S. A., Huenges, E. and Borm, G.: Estimating the crust permeability from fluid-injection-induced seismic emission at the KTB site, Geophysical Journal International, 131, (1997), 5–8.

Sibson, R. H.: Structural permeability of fluid-driven fault-fracture meshes. Journal of Structural Geology, 18, (1996), 1031–1042.

Valley, B. and Evans, K. F.: Stress magnitudes in the Basel enhanced geothermal system, International Journal of Rock Mechanics and Mining Sciences, 118, (2019), 1–20.

Wallace, R. E.: Geometry of Shearing Stress and Relation to Faulting, The Journal of Geology, 59(2), (1951), 118–130.

Watanabe, N., Hirano, N., and Tsuchiya, N.: Determination of aperture structure and fluid flow in a rock fracture by high-resolution numerical modeling on the basis of a flow-through experiment under confining pressure, Water Resource. Research, 44, (2008), 1–11.

Yeo, I. W., de Freitas, M. H., and Zimmerman, R. W.: Effect of shear displacement on the aperture and permeability of a rock fracture, International Journal of Rock Mechanics and Mining Sciences, 35(8), (1998), 1051–1070.

Zoback, M.;. Reservoir Geomechanics, Cambridge University Press, (2007).